ARTICLE

Continuous Flow Synthesis and Antimicrobial Evaluation of NHC* Silver Carboxylate Derivatives of SBC3 *in vitro* and *in vivo*

Received 00th January 20xx,
Accepted 00th January 20xx

DOI: 10.1039/x0xx00000x

Cillian O'Beirne, [†a] Magdalena E. Piatek,[b] Jen Fossen,[c] Helge Müller-Bunz,[a] David R. Andes,[c] Kevin Kavanagh,[b] Siddappa A. Patil,[d] Marcus Baumann,[a] Matthias Tacke[†a]

N-Heterocyclic silver carbene compounds have been extensively studied and shown to be active agents against a host of pathogenic bacteria and fungi. By incorporating hypothesised virulence targeting substituents into NHC-silver systems via salt metathesis, an atom efficient complexation process can used to develop new complexes to target the passive and active systems of a microbial cell. The incorporation of fatty acids and an FtsZ inhibitor have been achieved, and creation of both the intermediate salt and subsequent silver complex has been streamlined into a continuous flow process. Biological evaluation was conducted with *in vitro* toxicology assays showing these novel complexes had excellent inhibition against Gram-negative strains *E. coli*, *P. aeruginosa* and *K. pneumonia*; further studies also confirmed the ability to inhibit biofilm formation in Methicillin-resistant *S. aureus* and *C. Parapsilosis*. *In vivo* testing using a murine thigh infection model showed promising inhibition of MRSA for the lead compound **SBC3**, which is derived from 1,3-dibenzyl-4,5-diphenylimidazol-2-ylidene(NHC*).

Introduction

The need for new antimicrobial agents remains a priority for combating antimicrobial resistance.[1-3] Recent reports from both the Centre for Disease Control (CDC)[4] and United Nations (UN)[5] have highlighted the continuing cost in both life and national funds relating to this global problem, further emphasizing that new medicines are required to tackle a worldwide challenge that will claim up to 10 million lives per year by 2050.[5]

In this context, there has been an upsurge in the interest of utilizing metals as antimicrobial agents over the past several years.[8] Whilst there are comparatively few metal based antimicrobial treatments currently available, there exists a reservoir of extensively studied metal-based compounds that can be employed in the development of future clinical antimicrobials; be it as standalone compounds or in combination therapies[8,9] To this end, silver has a widely known usage as an antibiotic[10] and even some further reaching antimicrobial activity.[11,12] Interest in silver, past its use as a potent antimicrobial element in burn wound cream,[13] still remains high, with multiple different approaches still investigated for a way to exploit its multi-mechanistic action against a wide range of both pathogenic bacteria and fungi.[14-17] Further understanding of mechanism of action of silver against bacteria was recently reported by the Sun group;[18,19] by elucidating several definitive intracellular interactions between silver and essential enzymes in the glycolysis pathway in *E. coli*, silver now has at least one thoroughly defined mechanism of action that can be cultivated as a pathway in developing new metal-based antimicrobials.

Previous work by our group has shown that when coordinated to a suitable ligand, such as *N*-heterocyclic carbenes (NHCs), the transport and slow release of silver to a cell can be biologically facilitated, resulting in a silver-based antimicrobial capable of eliciting antibacterial effects[25] and even clinical level antifungal activity.[21] NHCs have a broad usage in both organometallic chemistry[22,23] and organic synthesis,[23] where tuning both the electronic and physiochemical properties of NHCs, allows for developing suitable biomolecules to combine with silver.[25-27]

Previous *N*-heterocyclic silver complexes have been synthesized by our group via either Youngs' method (using two parts silver acetate and an imidazolium salt),[20,26] or the widely exploited Arduengo method of generating a free carbene.[28] The Tacke group has produced a large suite of compounds by Youngs' method resulting in our most potent antimicrobial NHC-silver(I) complex to date.[20,26a] This has been matched in antimicrobial activity against several pathogenic strains (including MRSA) with several complexes made via the free carbene method.[21] It is now hoped to incorporate additional physiochemically enhancing, or possibly

[a] *School of Chemistry, University College Dublin, Belfield, Stillorgan, Dublin 4, Republic of Ireland.*
[b] *SSPC Pharma Research Centre, Department of Biology, Maynooth University, Maynooth, W23F2H6, Co. Kildare, Republic of Ireland.*
[c] *J. Fossen, Prof. D. R. Andes, Department of Medicine, 600 Highland Avenue, University of Wisconsin, Madison, USA.*
[d] *Centre for Nano and Material Sciences, Jain University, Bangalore, Karnataka, India.*
† Corresponding Authors: cillian.o-beirne@ucdconnect.ie; matthias.tacke@ucd.ie
Electronic Supplementary Information (ESI) available: See DOI: 10.1039/x0xx00000x

virulence factor targeting, substituents in order to see a marked improvement in activity against pathogenic microbial strains such as Methicillin-resistant *Staphylococcus aureus* (MRSA) and *Candida albicans*.[29,30] To realize more effective and scalable entries towards these important entities we wished to exploit continuous flow processing to streamline their assembly. Flow chemistry is widely recognized as a powerful technology for preparing simple building blocks and advanced structures in academia and industry alike.[31,32]

Commonly cited advantages such as improved heat and mass transfer derive from miniaturization of reactor components that consequently impart better process control, whilst continuous processing allows for increased scale and throughput. Furthermore, in continuous flow mode heterogeneous reagents can be incorporated via packed bed reactors to provide improved contact between substrate solution and reagent that in turn leads to faster and cleaner reactions.[33] Although a scarcity of examples that outline these principles in the context of organometallic synthesis are noted,[34] this work was encouraged by earlier reports from McQuade et al. and Willans et al., detailing the generation of NHC-copper species through use of flow synthesis.[35,36]

Herein, a novel route for the synthesis of several NHC-silver(I) complexes, containing previously hypothesized virulence factor targeting and intracellular protein targeting moieties, is demonstrated, including the subsequent flow synthesis in high yield and high purity. Several of these complexes were screened for biological activity against multiple pathogenic microbial species, including MRSA, using *in vitro* assays and *in vivo* methods including murine models.

Results and Discussion

Synthesis of complexes and adaptation to a flow synthesis

The investigation into a more desirable pathway for the creation of *N*-heterocyclic carbene silver(I) complexes had led to the creation of a more atom-efficient synthesis route. As Youngs' and Arduengo's methods for synthesizing previous compounds required long reaction times, have several side-products, result in moderate yields and, in the case of the free carbene pathway, require partial or full Schlenk conditions, it is desirable to realize a process that would eliminate these limitations.

Through the use of an anion exchange process we have generated several imidazolium salts (**1** – **6**, **8**) that can then be complexed with silver to produce the corresponding metal complex. The imidazolium salt precursor, 1,3-dibenzyl-4,5-diphenyl imidazolium bromide (given the shorthand of NHC*) was synthesized as per literature method.[26a] The imidazolium salt intermediates (**1** – **6, 8**) were achieved through use of a Vapourtec E-series flow reactor system in combination with Omnifit glass columns that were packed with the appropriate anion exchange resin.

The intermediate salts, **1** – **6** & **8**, were then produced by dissolving the NHC* imidazolium salt in methanol and passing it through a packed bed column containing the previously prepared exchange resin containing the newly desired anion (**Scheme 1**) and isolated in yields of 79 – 96%. Compound **7** that was not generated via the flow apparatus due to solubility issues within the flow system. This salt was synthesized in a benchtop procedure, using a biphasic dichloromethane/water solvent system and reacting sodium laurate with the NHC* precursor for 24 h.

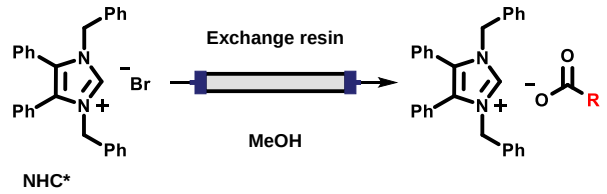

R = CH_3 / CF_3 / CH_2CH_3 / H / $CH_2(CH_2)_3CH_3$ / $CH_2(CH_2)_6CH_3$ / $CH{=}CHC_6H_5$

Scheme 1. Flow pathway of anion exchange

Having achieved the improved generation of these imidazolium salts (**1** – **8**), the corresponding NHC-silver(I) complexes were synthesized on the benchtop by reacting the respective salts with a stoichiometric amount of silver oxide, leaving only water as a by-product (**Scheme 2**).

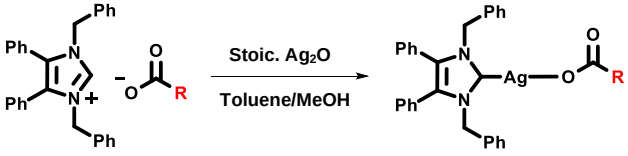

1 R = CH_3
2 R = CF_3
3 R = CH_2CH_3
4 R = H
5 R = $CH_2(CH_2)_3CH_3$
6 R = $CH_2(CH_2)_6CH_3$
7 R = $CH_2(CH_2)_9CH_3$
8 R = $CH{=}CHC_6H_5$

9 R = CH_3 (**SBC3**)
10 R = CF_3
11 R = CH_2CH_3,
12 R = H (**Impure**)
13 R = $CH_2(CH_2)_3CH_3$
14 R = $CH_2(CH_2)_6CH_3$
15 R = $CH_2(CH_2)_9CH_3$
16 R = $CH{=}CHC_6H_5$

Scheme 2. Synthesis of silver complexes **9** – **16**

The successful synthesis of complex **9**, given the moniker **SBC3**, via the new atom efficient pathway proved that this alternate method was applicable for creating other NHC-silver complexes. In addition to utilizing this new pathway, our attention turned to examining if it was possible to replace halogenated solvents, outright; previous complexes made by other routes have utilized halogenated solvents as the most effective medium for synthesis.[26a] In this new process, the chlorinated solvent dichloromethane is replaced by a greener alternative, namely toluene:methanol (3:1).[37]

This new method showed that complexes **9** - **16** can be obtained in an atom efficient way, on the benchtop, in good yields, 23 – 93%, requiring only minimal workup (**Table 1**). In this series of new NHC-silver complexes, the only compound that proved difficult to obtain in pure form was complex **12**, synthesized from the imidazolium salt containing a formate

anion. NMR spectroscopy confirmed the presence of the complex in 60% conversion, but elemental analysis proved the complex impure (See ESI).

During both the reaction and subsequent work up a silver mirror formed on two separate occasions. This comes as no surprise as formate can readily act as a reducing reagent to reduce silver to its elemental state.[38]

Now that this improved route was demonstrated, we wished to determine a way to increase the yield for all complexes. This was done was by utilizing an excess of silver oxide; this process proved successful, resulting in uniformly high yields of 82 – 93% (**Table 1**). Though high yields were obtained for all complexes, the long reaction time was still a challenge to be overcome. As the majority of the intermediate imidazolium salts were generated using a flow apparatus, a continuous flow process was designed to incorporate both the anion exchange and the silver complexation steps in a telescoped manner (**Scheme 3**).

Table 1. Yields of silver complexes using a) stoichiometric amounts of silver oxide and b) excess silver oxide; *See ESI for details

Complex	a) Stoic. Ag_2O Yield (%)*	b) Excess Ag_2O Yield (%)*
9	72	93
10	24	86
11	66	95
12	20	39
13	53	94
14	93	96
15	82	82
16	71	97

The anion exchange is performed via the same route as previously to generate the intermediate salts, with the eluent then fed combined with toluene to give a 3:1 toluene/methanol mixture, as is used in the benchtop synthesis. This solvent system containing the exchanged substrate is then pumped through a second column containing an evenly distributed mixture of silver oxide and activated 3 Å molecular sieves as a scavenger for water that is generated as a by-product.

The resulting product is collected in a covered flask that excludes light and the solvent then removed to give the NHC-Ag products in yields ranging from 73 to 98%. The longest total process time is 12 h for the total synthesis of complex **13** and shows a greater than six-fold decrease in overall reaction time from the standard 3 d benchtop synthesis.

The resulting product is collected in a covered flask that excludes light and the solvent then removed to give the NHC-Ag products in yields ranging from 73 to 98%. The longest total process time is 12 h for the total synthesis of complex **13** and shows a greater than six-fold decrease in overall reaction time from the standard 3 d benchtop synthesis.

Table 2 highlights the corresponding residence and processing times of the respective flow synthesis for each complex.

Table 2. Process time, residence time and final yield for the flow synthesis of NHC-Ag(I) complexes

Complex	Process time (h)	Residence time (min)	Yield (%)
9	4	17	98
11	8	35	97
12	8	35	73
13	12	26	86
14	6	26	93
16	8	35	99

Thus, by incorporating both the anion exchange and complexation steps into a single flow process reaction times were reduced significantly, while yields for several complexes increased by 2-5%. The synthesis of complex 12 was also telescoped using the total flow process in an attempt to circumvent the auto-reducing nature of the reaction. However, this proved unsuccessful with elemental analysis confirming an impure product, comparable to the product of the benchtop synthesis. The identity and purity of each complex was established using NMR and IR spectroscopy, and elemental analysis; see ESI for details.

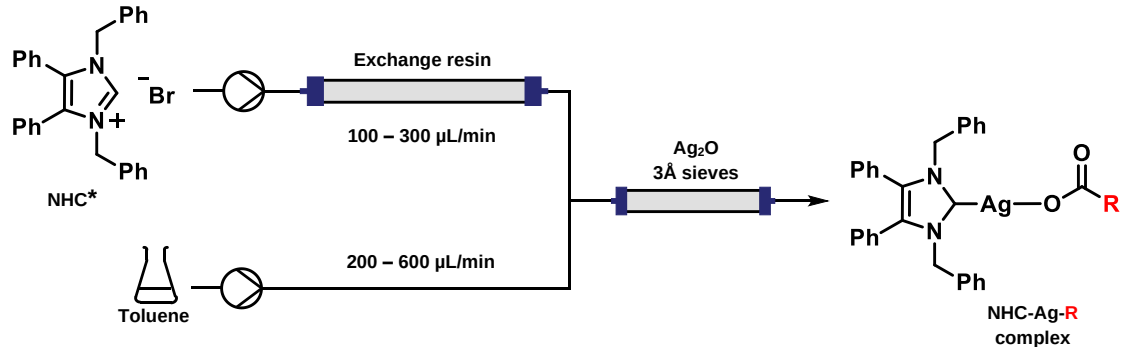

Scheme 3. Flow process for synthesis of NHC-silver(I) complexes

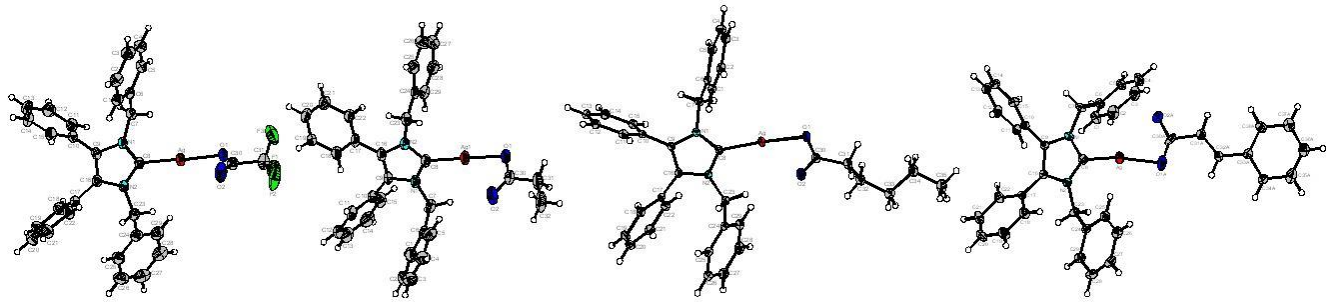

Figure 1. Molecular structures of complexes **10**, **11, 13** & **16**; thermal ellipsoids are drawn on the 50% level

The crystal structure of complex **10** was obtained by the slow diffusion of pentane into a super saturated solution of complex **10** in chloroform, and the crystal structures of complexes **11**, **13** & **16** were obtained by the slow diffusion of pentane into a super-saturated solution of the respective complex in dichloromethane (**Figure 1**). NHC-silver and silver-oxygen bond lengths, along with NHC-Ag- oxygen bond angles, correspond to previously reported values associated with this class of compounds.[21,26a]

The only outlier from the usually near-linear bond angles of these NHC-silver species is the bond angle of complex **16** at 165.33(12)° as seen before in this compound class.[39] In the crystallographic structure, two molecules of the compound are present within the unit cell and interactions between the bonding oxygen and silver atom of both molecules form a 4-coordination interaction in the dimer. This provides reason for the non-linear bonding between the silver and cinnamate moiety in the single molecule structure. This crystallographic data, bond angles and bond lengths can be found in the ESI.

In vitro & *in vivo* biological evaluation

Following on from the success of adapting the synthetic procedure to a flow system, several complexes were evaluated for antimicrobial activity.[20a] This activity of selected complexes were firstly demonstrated by *in vitro* toxicity assays against the selected bacterial strains of *E. coli*, *K. pneumoniae,* Methicillin-Resistant *S. aureus* (MRSA), *P. aeruginosa* and S. *aureus* (**Figures 2** & **3**).

The **SBC3** molecule, complex **9**, was chosen alongside its trifluoroacetate derivative (**10**) to determine the relative inhibition efficacies of these molecules and to set the base level activity for testing of future NHC-silver compounds. Two other compounds, **14** and **16**, containing previously hypothesized additional antimicrobial moieties, were also chosen for evaluation. Complex **14** incorporates a medium chain fatty acid with the aim of disrupting biofilm formation,[30] while complex **16** contains a confirmed FtsZ inhibitor moiety, shown previously to disrupt cell division in bacteria.[29]

SBC3 elicits the most potent activity against the Gram-negative species *E. coli*, *K. pneumoniae* and *P. aeruginosa*. Maximum growth inhibition (89%) was achieved against *K. pneumoniae* at a concentration of 62.5 µg/mL, and *E. coli* (86%) at the 15.63 µg/mL concentration. The complex also demonstrated good activity against Gram-positive species, reducing MRSA growth by 74% at the 31.25 µg/mL concentration (**Figure 2**).

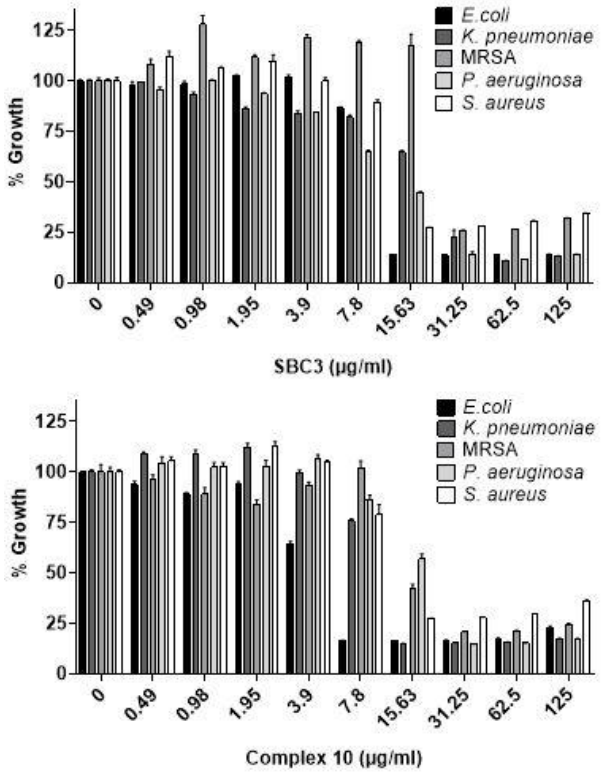

Figure 2. Antibacterial evaluation of complexes **9** (**SBC3**) & **10**

Complex **10** significantly reduced *E. coli* growth from 86% to 16% at 7.8 µg/mL. *K. pneumoniae* was also more susceptible at lower concentrations with 85% inhibition at 15.63 µg/mL. A lower dose of complex **10** (15.63 µg/mL) reduced *S. aureus* growth by 73%, having a similar effect as **SBC3** on MRSA with 79% inhibition at 31.25 µg/mL (**Figure 2**).

Complex **14**, containing the nonanoate moiety, exhibited excellent inhibition (86%) against *E. coli* at a concentration of

7.8 µg/mL, whilst also showing 84% and 87% inhibition versus *P. aeruginosa* and *K. pneumoniae* at the 15.63 µg/mL concentration, respectively. At the same concentration, *S. aureus* and MRSA were inhibited by approximately 50% (**Figure 3**).

The antimicrobial activity of complex **16**, containing the cinnamate FtsZ inhibitor moiety, remained consistent with previous findings showing greatest activity against Gram-negative species, particularly against *E. coli*, reducing growth by 82% at 15.63 µg/mL. This complex also showed activity against the Gram-positive strains with 76% inhibition against MRSA at 62.5 µg/mL (**Figure 3**).

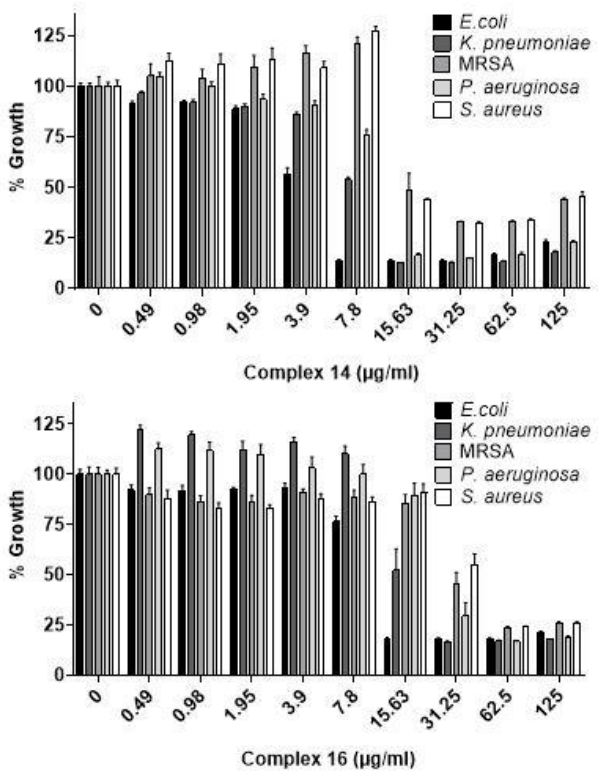

Figure 3. Antibacterial evaluation of complexes **14** & **16**

Two pathogenic fungal species, *C. albicans* and *C. parapsilosis*, were also screened for antifungal alongside the selected bacteria. *Candida* species are among the most prevalent causes of fungal infection in immunocompromised individuals[40,41] and previous publications have shown preferential activity of NHC-silver complexes against both strains, providing an opportunity to confirm a continuous broad spectrum activity of this compound class against clinically relevant fungal pathogens.[21]

All complexes show good inhibition against *C. parapsilosis* with complex **10** showing 77% inhibition at 7.8 µg/mL concentration and complex **14** showing similar inhibition at the 15.63 µg/mL concentration. **SBC3** showed less activity against *C. parapsilosis*, but still maintained 60% inhibition at the 15.63 µg/mL concentration. **SBC3** and complex **14** showed inhibition of *C. albicans* but only at high concentrations (62.5 – 125 µg/mL), with complex **10** showing little to no inhibition, even at high concentrations.

Testing of complexes **14** & **16** highlighted a more pronounced inhibitory effect of both strains of *Candida albicans* compared to **SBC3** and complex **10**, with 95% inhibition shown at 62.5 µg/mL (Complex **14**) and 94% at 125 µg/mL (Complex **16**).

Complex **10** resulted in 90% inhibition of *C. parapsilosis* at 31.25 µg/mL, and an increased dose of 62.5 µg/mL reduced growth by 85% (complex **14**) and 88% (complex **16**). Previous research by Browne et al.,[20a] focused on the activity of **SBC3** against *C. albicans* where about 86% growth inhibition was achieved at a concentration of 25 µg/mL. Although this current study did not reach this same level of success in treating *C. albicans*, the results obtained for *S. aureus* were comparable (about 71% at 25 µg/mL); See ESI for additional graphical data.

The overall inhibition of cell growth ascertains a compounds effect as an antimicrobial agent; however this does not give specific insights into its mode of action. To supplement the activity shown by the complexes tested, the effect on the specific inhibition of biofilms was measured.[42] Biofilms are important virulence factors in many bacterial and fungal species, playing key roles in adhesion and allowing microbial colonies to form and grow.[43,44] As biofilms represent an important infection process, the previously chosen complexes were screened to determine if there is specific biofilm inhibition against *P. aeruginosa*, MRSA and *C. parapsilosis*.

The treatment of *P. aeruginosa* with selected complexes showed no significant inhibition of biofilm in all concentration ranges. However, treatment of MRSA and *C. parapsilosis* did result in significant growth inhibition (**Figures 4** & **5**); all further inhibition results can be found in the ESI.

Against MRSA, it can be seen that all complexes have an inhibitory effect on biofilm formation at the higher concentrations tested. At the higher cell density of OD = 0.1, the standout activity is shown by complexes **10** and **16**, with 50% inhibition achieved at 2 µg/mL concentration. This result is interesting as the medium length fatty acid chain of the complex **14** was hypothesized to be the better biofilm disruptor,[30] and this is seen in the lower cell concentration assay at OD = 0.01, whoever complexes **10** and **16** have shown greater activity at the higher cell concentration (**Figure 4**).

Against *C. parapsilosis*, **SBC3** and complex **14** show the greater activity against fungal cells at the higher cell concentration of OD = 0.1. **SBC3** inhibits up to 75% biofilm growth at 4 µg/mL, while complex **14** inhibits up to 50% growth at the same concentration (**Figure 5**).

The results of this screening have shown that there is definitive inhibition of biofilms in MRSA and *C. parapsilosis* by select complexes. The inhibition of MRSA biofilms highlights targeting virulence factors in resistant pathogens as a feasible option with this compound class.

While the previously hypothesized "biofilm disruptor" moieties like fatty acids showed better activity against *C. parapsilosis*, the use of more lipophilic or other cellular targeting modalities like that of the FtsZ inhibiting cinnamate

may be the more poignant groups for further investigation in treating MRSA.

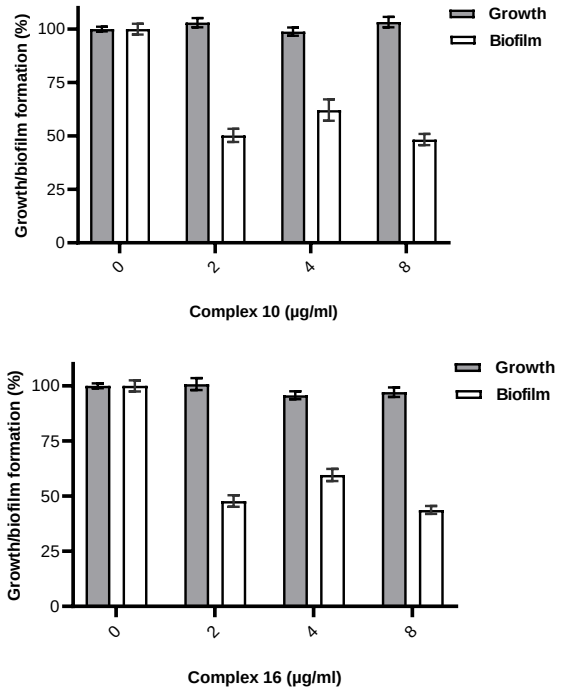

Figure 4. Inhibition of MRSA biofilms by complexes **10** & **16**; "Growth" portrays overall growth of bacterial cells, "Biofilm" portrays biofilm growth to highlight specific inhibition of biofilm; cell concentration: OD = 0.1

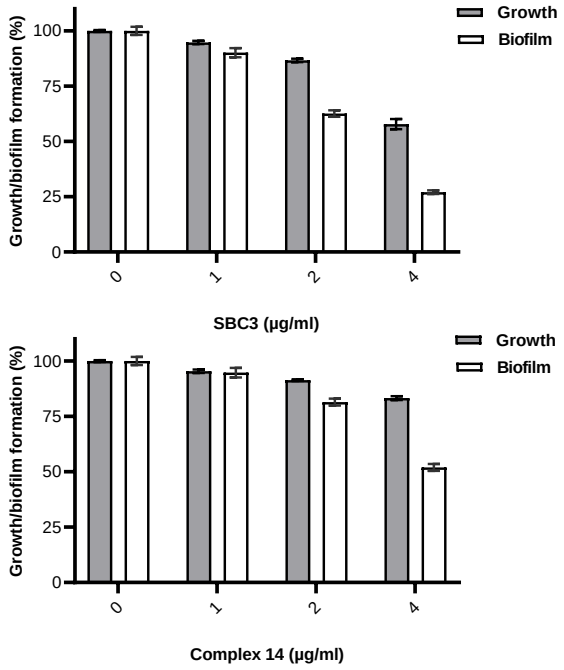

Figure 5. Inhibition of *C. parapsilosis* biofilms by **SBC3** & complex **14**; "Growth" portrays overall growth of bacterial cells, "Biofilm" portrays biofilm growth to highlight specific inhibition of biofilm; cell concentration: OD = 0.1

To gain a more complete picture of the antibiotic activity of this class of compounds, an *in vivo* murine thigh infection model was used to determine the activity of **SBC3** and complex **10** against a strain of MRSA (ATCC 33591).[45,46]

Both complexes had previously shown good activity against the spread of bacterial and fungal pathogens, and inhibition of biofilms, and were decided these were the more ideal compounds for murine testing; this would also allow investigating if the incorporation of the trifluoromethyl group on the acetate moiety, and the theorized greater lipophilicity, would lead to a noticeable increased antibiotic activity in an *in vivo* environment.

Two separate dosing regimens were carried out to determine the dosages that were effective for antibiotic efficacy, while also remaining tolerable to the infected mice. The results of this testing are represented in **Figure 6**.

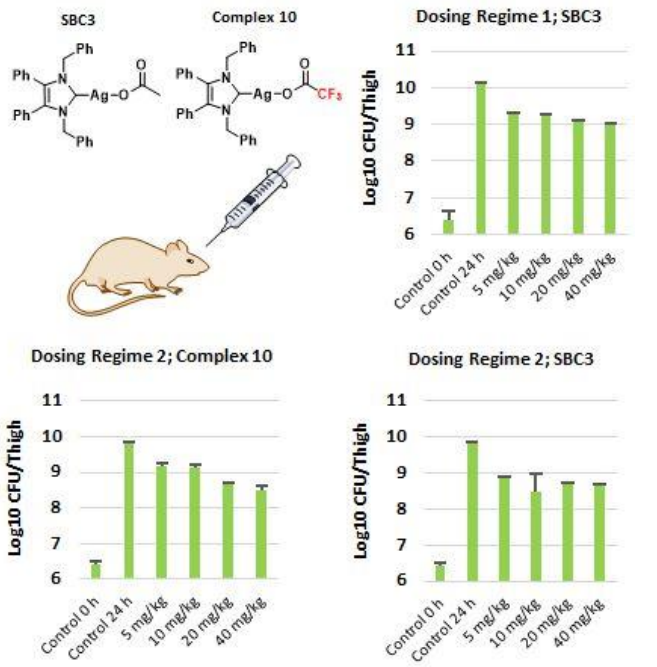

Figure 6. *In vivo* murine thigh-infection model on the efficacy of **SBC3** and Complex **10** against MRSA

In the first regime, **SBC3** was administered in a standalone test to determine the tolerability of the complex by the murine subjects. The MRSA-related $\log_{10}$ CFU/thigh values were measured for the control group at 0 h and at 24 h, respectively. Dosages **SBC3** were administered in concentrations of 5, 10, 20 and 40 mg/kg; the mice were monitored over a 24 h period. As seen in **Figure 7**, there is a consistent concentration-dependent lowering of MRSA-related CFU, with no toxicity.

The second regime of testing included both **SBC3** and complex **10**, with a change of dosage amount from every 12 h to every 6 h, doubling the dose received by the mice. For this regime, the MRSA-related $\log_{10}$ CFU/thigh values were measured for the control group at 0 h and at 24 h,

respectively. Dosages of the **SBC3** molecule and complex **10** were administered in concentrations of 5, 10, 20 and 40 mg/kg; the mice were monitored over a 24 h period.

At the 5 mg/kg and 10 mg/kg concentrations, there is a similar decrease in the MRSA-related $\log_{10}$ CFU/thigh values for the corresponding dosages of **SBC3** and complex **10**. Whilst a definitive decrease in MRSA-related $\log_{10}$ CFU is shown, the effects are still not as pronounced as would be expected for a clinical antimicrobial. At the higher concentration ranges of 20 mg/kg and 40 mg/kg, there is also further increased activity; however, these concentrations resulted in toxicity issues for both **SBC3** and complex **10,** with all mice in these test sub-groups dying during treatment. This new data has highlighted a different avenue of use should be considered for this class of antimicrobial complexes, most notably as adjuvants for previously resisted clinical antimicrobials.

Conclusions

The use of silver as an antimicrobial has long been explored by researchers for new medicines and as a possible avenue for undermining resistance against clinical antimicrobial agents. The combination of silver with ligands capable of providing a delivery system to bacterial and fungal cells to elicit its effects has been a well examined route of previously developing biologically active complexes; *N*-heterocyclic carbenes provide suitable scaffolds for this purpose. The incorporation of physiochemically improving and virulence factor targeting carboxylate substituents then provide the opportunity to improve the antimicrobial efficacy of these complexes, by both the direct attack on microbial cells and subversively attacking the attributes that make them effective pathogens. To this end we have developed a unique method for the synthesis of NHC*-Ag complexes by first creating intermediate imidazolium salts, that contain unique carboxylate groups via an anion exchange procedure, and a direct method for complexation with silver that leaves only water as a by-product to obtain NHC*-Ag complexes in high yields.

In addition to this, we then successfully incorporated the salt metathesis and subsequent silver complexation to a single, continuous flow process, reducing the reaction time from a period of days down to hours, whilst achieving improved yields with several compounds.

The biological examination of these compounds has elucidated a clear outcome for these NHC*-Ag complexes. The resulting effect during *in vitro* tests has shown good activity against the Gram-negative bacterial strains *E. coli*, *K. pneumoniae* and *P. aeruginosa*, with the effect of complexes **10** and **14** (containing a trifluoroacetate and medium length fatty acid, respectively), resulting in excellent inhibition (>75%) against *E. coli* at the concentration of 7.8 µg/mL. The findings of antifungal assays have also highlighted the continued activity of this compound class against *C. parapsilosis*, with complexes **10** and **14** again providing more than 50% inhibition against this fungus at the concentration of 7.8 µg/mL.

To try and elucidate a mechanism by which this compound class elicits microbial growth inhibition, the four selected complexes were screen for their ability to inhibit biofilm formation. As biofilm is a necessary virulence factor in the development of many pathogenic bacteria and fungi, particularly MRSA, this represented a clear target for increasing antibiotic activity. Biofilm inhibition was achieved against *C. parapsilosis* at the lower concentrations by **SBC3** and complex **14**, with complexes **10** and **16** showing the greatest inhibition of MRSA biofilms at a concentration of 2 µg/mL.

The resulting murine model also highlighted the extent of inhibition for this compound class against the resistant Gram-positive strain MRSA in an *in vivo* environment. The complexes tested, **SBC3** and complex **10**, produced a definitive decrease in the presence of MRSA related cells in mice, though toxicity issues present a problem in an increased dosage regime where the greater effect was witnessed. These murine results show a certain activity of **SBC3** and **10** *in vivo*, but for a hit compound a significantly higher bacterial load reduction of 2-3 orders of magnitude could be expected.

These results highlight that the standalone activity of this class of NHC*-Ag compounds may not be sufficient to clinically treat microbial infections. To this end, we see this class of complexes as supplementary adjuvants to frontline antimicrobial agents. As antimicrobial research has more gradually turned towards combination therapies and adjuvants as useful tools,[47] these compounds could be utilized as a resistance undermining element in a combination therapy in order to re-establish the effect of clinically relevant antimicrobials.[9,48] Recently, Rubini et al. have published a study on the antibacterial mechanism of action of **SBC3,** whilst also showing its effect as an antibacterial adjuvant for Gentamicin against resistant strains of *P. aeruginosa*.[49]

In tandem with the ability of being able to synthesise NHC*-Ag complexes in an eco- and industry friendly continuous flow system, we have shown that these latest complexes can be suitably derivatised with more biologically active scaffolds and are appropriately robust to be created in high yields and purity. Together with the *in vivo* data presented, there is now a greater likelihood to see clinical trials of an advanced carbene silver antimicrobials in the foreseeable future.

Experimental Section

Please see ESI for full synthesis and biological assay details.

Conflicts of interest

There are no conflicts to declare.

Acknowledgements

We would like to thank the School of Chemistry & the College of Science of University College Dublin for the funding to achieve these research findings. The authors thank UCD, Systems Biology Ireland (SBI) for access to the Agilent 6546 QTOF system, which is part of the CMAP initiative and was

funded under 18/RI/5702 Science Foundation Ireland Infrastructure (SFI) Call 2018. This work was also supported by funding from a research grant from Science Foundation Ireland (SFI) and is co-funded under the European Regional Development Fund under grant number 12/RC/2275_P2.

Notes and references

1 A. Frei, J. Zuegg, A. G. Elliot, M. Baker, S. Braese, C. Brown, F. Chen, C. G. Dowson, G. Dujardin, N. Jung, A. P. King, A. M. Mansour, M. Massi, J. Moat, H. A. Mohamed, A. K. Renfrew, P. J. Rutledge, P. J. Sadler, M. H. Todd, C. E. Willans, J. J. Wilson, M. A. Cooper and M. A. T. Blaskovich, *Chem. Sci.*, **2020**, 11, 2627-2639.

2 C. Molina-Santiago, A. de Vincente and D. Romero, *Microb. Biotechnol.*, **2017**, 11, 976-978.

3 C. L. Ventola, *Pharm. Ther.*, **2015**, 40, 277-283.

4 CDC. Antibiotic Resistance Threats in the United States, 2019.; U.S. Department of Health and Human Services, CDC; Atlanta, GA; **2019**.

5 WHO. No Time to Wait: Securing the future from drug-resistant infections; Report to the Secretary-General of the United Nations. **2019**.

6 G. Barlow, *Nat. Microbiol.*, **2018**, 3, 258–260

7 Theuretzbacher et al., *J. Antimicrob. Chemother.,* **2015**, 70, 2177–2181.

8 A. Frei, *Antibiotics*, **2020**, 9, 90.

9 M. A. Sierra, L. Casarrubios and M. C. de la Torre, *Chem. Eur. J.,* **2019**, 25, 7232-7242.

10 W. Sim, R. T. Barnard, M.A. T. Blaskovich and Z. M. Ziora, *Antibiotics*, **2018**, 7, 93.

11 R. Morones-Ramirez, J. A. Winkler, C. S. Spina and J. J. Collins, *Sci. Transl. Med.,* **2013**, 5(190), 190ra81.

12 L. Zou, J. Want, X. Ren, L. Zhang, M. E. Rottenberg and A. Holmgren, *EMBO Mol. Med.*, **2017**, 9, 1165–1178.

13 A. Melaiye and W. J. Youngs, *Expert Opin. Ther. Patents*, **2005**, 15, 125-130.

14 G. Wan, L. Ruan, Y. Yin, T. Yang, M. Ge and X. Cheng, *Int. J. Nanomed.*, **2016**, 11, 3789-3800.

15 N. Xu, H. Cheng, J. W. Xu, F. Li, C. Gao, K. F. Huo, J. J. Fu, Q. Xiong, *Int. J. Nanomed.,* **2017**, 12, 731-743.

16 D. Armstrong, S. M. Kirk, C. Murphy, A. Guerriero, M. Peruzzini, L. Gonsalvi and A. D. Philips, *Inorg. Chem.,* **2018**, 57, 6309-6323.

17 S. Medici, M. Peana, G. Crisponi, V. M. Nurchi, J. I. Lachowicz, M. Remelli and M. A. Zoroddu, *Coord. Chem. Rev.* **2016**, 327-328, 349-359.

18 H. Wang, M. Wang, X. Yang, X. Xu, Q. Hao, A. Yan, M. Hu, R. Lobinski, H. Li and H. Sun, *Chem. Sci.* **2019**, 10, 7193-7199.

19 H. Wang, A. Yan, Z. Liu, Z. Yang, Z. Xu, Y. Wang, R. Wang, M. Koohi-Moghadam, L. Hu, W. Xia, H. Tang, Y. Wang, H. Li and H. Sun, *PLoS Biol.,* **2019**, 17, e3000292.

20 a) N. Browne, F. Hackenberg, W. Streciwilk, M. Tacke and K. Kavanagh, *Biometals*, **2014**, 27, 745–752; b) C. R. Shahini, G. Achar, S. Budagumpi, H. Müller-Bunz, M. Tacke and S. A. Patil, *J. Organomet. Chem.*, **2018**, 868, 1-13; c) C. R. Shahini, G. Achar, S. Budagumpi, M. Tacke and S. A. Patil, *Inorg. Chim. Acta*, **2017**, 466, 432–441; d) A. Patil, S. A. Patil, R. Patil, R. S. Keri, S. Budagumpi, G. R. Balakrishna and M. Tacke, *Fut. Med. Chem.*, **2015**, 7, 1305–1333; e) M. A. Sharkey, J. P. O'Gara, S. V. Gordon, F. Hackenberg, C. Healy, F. Paradisi, S. Patil, B. Schaible and M. Tacke, *Antibiotics*, **2012**, 1, 25 - 28.

21 C. O'Beirne, N. F. Alhamad, Q. Ma, H. Müller-Bunz, K. Kavanagh, G. Butler, X. Zhu and M. Tacke, *Inorg. Chim. Acta*, **2019**, 486, 294-303.

22 M. G. Gardiner and C. C. Ho, *Coord. Chem. Rev.,* **2018**, 375, 373-388.

23 S. Y. Hussaini, R. A. Haque and M. R. Razali, *J. Organomet. Chem.,* **2019**, 882, 96-111.

24 D. M. Flanigan, F. Romanov-Michailidis, N. A. White and T. Rovis, *Chem. Rev.*, **2015**, 115, 9307-9387.

25 A. Kascaan-Nebioglu, M. J. Panzner, C. A. Tessier, C. L. Cannon and W. J .Youngs, *Coord. Chem. Rev.* **2007**, 251, 884-895.

26 a) S. Patil, A. Deally, B. Gleeson, H. Müller-Bunz, F. Paradisi and M. Tacke, *Metallomics*, **2011**, 3, 74–88; b) I. Fichtner, D. Behrens, J. Cinatl jr., M. Michaelis, L. C. Sanders, R. Hilger, B. N. Kennedy, A. L. Reynolds, F. Hackenberg, G. Lally, S. J. Quinn, I. McRae and M. Tacke, *Lett. Drug Des. Discov.,* **2012**, 9, 815-822.

27 N. A. Johnson, M. R. Southerland and W. J. Youngs, *Molecules*, **2017**, 22, 1263.

28 A. J. Arduengo, R. L. Harlow and M. Kline, *J. Am. Chem. Soc.,* **1991**, 113, 361-363.

29 S. Tripathy and S. K. Sahu, *Bioorg. Chem.,* **2019**, 91, 103169.

30 P. Y. Chung and Y. S. Toh, *Pathog. Dis.,* **2014**, 70, 231-239.

31 J. Britton and C. L. Raston, *Chem. Soc. Rev.,* **2017**, 46, 1250-1271.

32 a) A. Adamo et. al., *Science*, **2016**, 352, 61-67; b) M. Baumann, T.S. Moody, M. Smith and S. Wharry, *Org. Process Res. Dev.*, **2020**, doi.org/10.1021/acs.oprd.9b00524; c) A. Gioiello, A. Piccinno, A.M. Lozza and B. Cerra, *J. Med. Chem.,* **2020**, 63, 6624-6647; d) E. Lopez, M. L. Linares and J. Alcazar, *Future Med. Chem.,* **2020***,* doi.org/10.4155/fmc-2020-0075M.

33 B. Plutschack, B. Pieber, K. Gilmore and P. H. Seeberger, *Chem. Rev.*, **2017**, 117, 11796−11893.

34 J. Zhang, C. Gong, Z. Zeng and J. Xie, *Coord. Chem. Rev.*, **2016**, 324, 39-53.

35 S. M. Opalka, J. K. Park, A. R. Longstreet and D. Tyler McQuade, *Org. Lett.*, **2013**, 15, 996–999.

36 M. R. Chapman, Y. M. Shafi, N. Kapur, B. N. Nguyen and C. E. Willans, *Chem. Commun.*, **2015**, 51, 1282-1284.

37 D. Prat et al., *Org. Process Res. Dev.*, **2013**, 17, 1517−1525.

38 L. Jeong and W. H. Park, *Int. J. Mol. Sci.*, **2014**, 15, 6857-6879.

39 C. O'Beirne, H. T. Althani, O. Dada, J. Cassidy, K. Kavanagh, H. Müller-Bunz, Y. Ortin, X. Zhu and M. Tacke, *Polyhedron*, **2018**, 149, 95–103.

40 D. Trofa, A. Gácser and J. D. Nosanchuk, *Clin. Microbiol. Rev.,* **2008**, 21, 606-625.

41 M. A. Kabir and Z. Ahmad, *ISRN Prev Med.*, **2013**, 2013, 763628.

42 G. A. O'Toole, *J. Vis. Exp.,* **2011**, 47, 2437.

43 M. Cavalheiro and M. C. Teixeira, *Front. Med.,* **2018**, 5, 28.

44 K. M. Craft, J. M. Nguyen, L. J. Berg and S. D. Townsend, *Med. Chem. Commun.*, **2019**, 10, 1231.

45 National Research Council, Committee on the Care and Use of Laboratory Animals, Institute of Laboratory Animal Resources, Commission on Life Sciences, **1996**, Guide for the care and use of laboratory animals. National Academy Press, Washington, DC.

46 D. Andes and W. A. Craig, *Int. J. Antimicrob. Agents*, **2002**, 19, 261–268.

47 a) Y. Liu, R. Li, X. Xiao and Z. Wang, *Crit. Rev. Microbiol.*, **2019**, 45, 301; b) H. Douafer, V. Andrieu, O. Phanstiel IV and J. M. Brunel, *J. Med. Chem.*, 2019, 62, 8665-8681.

48 F. Barras, L. Aussel and B. Ezraty, *Antibiotics*, **2018**, 7, 79.

49 J. O'Loughlin, S. Napolitano, F. Alkhathami, C. O'Beirne, D. Marhöfer; M. O'Shaughnessy; O. Howe, M. Tacke, M. Rubini, *ChemBioChem*, **2021**, doi.org/10.1002/cbic.202000707.

